Numerical Simulation of Gas−Solid Dynamics in a Circulating Fluidized-Bed Riser with Geldart Group B Particles

ARTICLE *in* INDUSTRIAL & ENGINEERING CHEMISTRY RESEARCH · NOVEMBER 2007

Impact Factor: 2.59 · DOI: 10.1021/ie0700819

2 AUTHORS:

S. Vaishali
SunEdison
11 PUBLICATIONS **57** CITATIONS
SEE PROFILE

Shantanu Roy
Indian Institute of Technology Delhi
81 PUBLICATIONS **717** CITATIONS
SEE PROFILE

Numerical Simulation of Gas−Solid Dynamics in a Circulating Fluidized-Bed Riser with Geldart Group B Particles

S. Vaishali and Shantanu Roy*

Department of Chemical Engineering, Indian Institute of Technology−Delhi, Hauz Khas, New Delhi 110016, India

Satish Bhusarapu, M. H. Al-Dahhan, and M. P. Dudukovic

Chemical Reaction Engineering Laboratory, Department of Energy, Environment & Chemical Engineering, Washington University, Campus Box 1198, St. Louis, Missouri 63130-4899

Circulating fluidized-bed (CFB) risers with Geldart group B particles have found significant application in combustion reactions. The present work attempts to study the solids flow dynamics in a CFB riser that is operated with group B particles, using computational fluid dynamics (CFD) techniques. The key feature in the present study is that the various closure schemes in the CFD model have been evaluated against data from non-invasive experimental techniques: computer automated radioactive particle tracking (CARPT) for solids velocity field and computed tomography (CT) for solids holdup. Since solids flow in a riser is *multiscale* in character, in addition to the measured averaged solids velocity profiles and solids fraction profiles in the experimental section, mean granular temperature profiles have also been compared. Two flow regimes (viz., fast fluidization and dilute phase transport) have been considered in this study.

1. Introduction

A circulating fluidized-bed (CFB) riser is a "short contact time" reactor, in which solids (catalyst or one of the reactants) are fluidized at velocities higher than the characteristic "transport velocity", so that they are entrained out of the bed. To maintain a steady-state circulation and prevent the loss of expensive catalytic material, the solids are recycled back after regeneration. This closed-loop configuration offers several advantages,[1] such as void free operation, excellent heat and mass transfer, good gas−solids contact, high throughput rates per unit area, and optimal contact times. Therefore, CFBs find application in various fields such as calcination operations, the combustion of coal and other varieties of solid fuels, fluid catalytic cracking, ore roasting, the partial oxidation of lighter alkanes, and polyethylene production.

Although CFB technology was commercialized in the 1970s, our knowledge about the dynamics of gas−solid flow fields and structures therein is limited. Currently, the design of an industrial CFB reactor relies largely on empirical relationships and prior experience, and the interactions of the flow field dynamics with the catalytic chemistry. Clearly, this offers opportunities to enhance the performance of the reactor via the systematic investigation of the flow structure.

In the last few decades, computational fluid dynamics (CFD) has become one of the efficient tools for modeling multiphase systems such as bubble columns,[2] bubbling fluidized beds,[3,4] spouted beds,[5] and CFB risers,[6,7] at laboratory scales as well as pilot-plant scales. Most of the earlier CFD modeling work, in the case of CFB risers,[7−9] have been done for fluid catalytic cracking (FCC). FCC risers[1] typically involve catalyst particles that belong to Geldart group A,[10] in regard to their classification, and are operated at velocities in the range of 8−18 m/s and solids mass flux of 400−1400 kg/m^{2}s. In addition to FCC, the other very important application area for risers is the combustion of various fuels (coal, lignite, palletized solid biomass, etc.). In fact, by the end of the past decade, ∼500 CFB combustion units were operational worldwide.[11] A typical CFB combustor[1] consists of Geldart[10] group B particles with comparatively lower operating velocity (5−9 m/s) and solids mass flux (10−100 kg/m^{2}s).

For high velocity flows, such as that in a riser, group A particles exhibit higher slip velocity (∼25−30 times greater than the single particle terminal velocity, Yerushalmi and Avidan[12]), which is the probable cause of metastable structures (also called as "clusters") in the reactor. Being of higher "effective mass", they enhance the "slip" between the phases and render the multiphase flow field remarkably complex. Therefore, most of the research in the case of fast flows with group A particles has been focused on the formation and dissolution of clusters, and their effect on the overall dynamics.[13] In the case of CFB with group B particles,[14] slip velocities are in the range of the single particle terminal velocity (only ∼2−3 times greater) and, consequently, exhibit more-uniform flow. In group A particles, the minimum bubbling velocity is much higher than the minimum fluidization velocity, and a stable bubble size exists. In the case of group B particles, the minimum bubbling velocity is equal to the minimum fluidization velocity and a stable bubble does not exist. Molerus[15] noted that, in contrast to Geldart[10] group A particles, group B particles have negligible adhesive forces, in comparison to the drag force. Using dimensional analysis, Peirano et al.[16] has shown that in Geldart[10] group A and B, particles show significant differences in their response to gas-phase turbulence, energy dissipation mechanism, granular pressure and temperature dependence, and transition from a dense regime to a dilute regime.

Quite clearly, the hydrodynamic behavior of group B particles is expected to be distinctly different from that of group A particles, even when in the riser or standpipe flow. Indeed, this has been experimentally shown by Bhusarapu,[17] as well as others (Tsuji et al.,[18] Luo,[19] Mathiesen et al.,[20] and Ibsen et al.[21]). However, particularly on the theoretical modeling front, very

* To whom correspondence should be addressed. Tel.: 91-11-2659 6021. Fax: 91-11-2658 1120. E-mail address: roys@chemical.iitd.ac.in.

10.1021/ie0700819 CCC: $37.00
Published on Web 11/06/2007

few CFD modeling studies have been reported in the past for CFB units with group B particles. Notable among the reported studies is the work of Ibsen et al.,[21] who investigated the fluid flow in a complete CFB unit operated with group B particles. In this study, the radial and axial solids velocity profiles predicted by the CFD model were validated using one-dimensional (1-D) laser and phase doppler anemometry measurements. It was reported that Syamlal and O'-Brien's[22] drag closure predicted the solids velocity better than the conventionally used Wen and Yu's[23] drag closure. However, the CFD model was based on several assumptions, and rigorous validation of the model was not presented. Nieuwland et al.[24] developed a more-advanced two-dimensional (2-D) fluid model for group B sand particles, based on the *two-fluid modeling concept*, taking into account the kinetic transport mechanism in the particulate phase. Validation experiments were performed using reflective optical probes. Although the developed model offered improvements over the earlier Ding and Gidaspow[3] model, it underpredicted the experimentally observed centerline solids velocity and was not able to predict the solids segregation with fidelity. Also, the slip velocity that was predicted by Nieuwland et al.[24] was greater (~4−5 times) than the single particle terminal velocity. Zhang and Reese[25] developed a two-fluid model with isotropic gas turbulence for group B riser flow. This model exhibited uniform solids distribution at walls, when compared to the experimental data.

The current state-of-the-art picture in gas−solids dispersed flow in risers with Geldart[10] group B particles is rather confusing and incomplete. The lack of clarity partially results from the lack of comprehensive validation of the presented CFD models. Also, the multitude of closure forms and CFD modeling approaches available for gas−solids flow make the choice difficult for the practitioner, unless adequate experimental validation points toward a particular combination of modeling approach, conservation equations, closure forms, and numerical schemes.

In this contribution, we make an attempt in that direction by validating a CFD model of Geldart[10] group B particulate flow in a gas−solids riser with experimental results determined by computer automated radioactive particle tracking (CARPT) and computed tomography (CT) measurements. Furthermore, we report the comparisons of model predictions with second-order moments of velocity fluctuations.

2. Summary of Experimental Work

In the present work, the modeling is presented for the CFB unit at the Chemical Reaction Engineering Laboratory (CREL) at Washington University, St. Louis, MO.[17] The CREL CFB riser setup (Figure 1) is 7.9 m high and has an internal diameter of 15.2 cm; it is used for low-solid-mass-flux conditions (less than 100 kg/m^{2}s). CARPT studies on this setup were conducted in a section that was considered to be fully developed in a time-averaged sense at an axial height that varied from $Z = 4.6$ m to 5.85 m. γ-ray tomography experiments were performed at $Z = 5$ m and $Z = 5.47$ m, which fall within the zone of investigation of the CARPT experiments. The riser was operated in two commonly observed flow regimes, viz. fast fluidization (FF) and dilute phase transport (DPT). As reported by Bhusarapu,[17] the FF regime is characterized by axial solids segregation and exhibit a net downflow of solids at the wall, whereas the DPT regime exhibits more-uniform upflow of solids.

Details of the experimental techniques and results are presented elsewhere.[17,26,27] Here, only a brief discussion is presented, for the sake of completeness, and the details particularly relevant to the CFD calculations are highlighted.

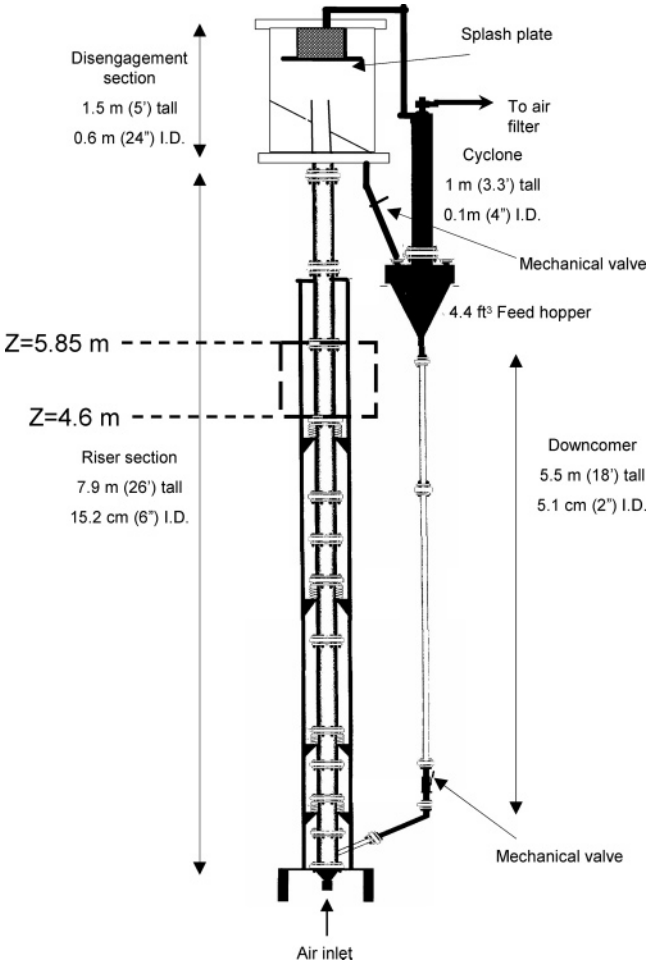

Figure 1. Schematic diagram of the CREL riser with a computer automated radioactive particle tracking (CARPT) zone of investigation.

CARPT is based on the principle of tracking the motion of a single tracer particle as a marker of the dispersed phase (solids in the case of a gas−solid riser). In the case of the gas−solids riser experiment, the solid phase was tagged with a ^{46}Sc γ-ray source (half-life = 83 days, density = 3000 kg/m^3). The 136-μm scandium particle was coated with ParyleneN polymer to make the tracer particle have the same size and density as that of the solids (i.e., 150 μm and 2550 kg/m^3) and prevent it from possible attrition upon collision with the walls and the other particles. Subsequent motion of this tracer particle was monitored using an array of 18 strategically placed scintillation detectors over a long time span in which the tracer visits each location in the zone of investigation a large number of times. To precisely determine the entry and exit time of the radioactive tracer in the zone of investigation, two "sentry detectors" were placed at the entrance and exit of the CARPT section, to record the entry and exit of the tracer particle from the zone of interrogation. Figure 1 shows the schematic diagram of the CREL riser with an axial zone of investigation for CARPT experiments. Typically, the total number of occurrences of the tracer in the section investigated varied from 0.8 million to 1.75 million. A record of the γ-ray photon counts at each detector location and tracer particle location was used to reconstruct the precise particle position at each time instant. One of the unique features of the current CARPT experiment was that, for the first time, it was implemented on a relatively fast system (earlier work was related mostly to gas−liquid and liquid−solid systems

with mean velocities well below 1 m/s[26,28,29]), which demanded higher data acquisition frequency (200 Hz in the current experiment, versus 50 Hz in previous experiments). In addition, very similar to the previous work of Roy et al.,[26] this work involved the tracer particle repeatedly entering and exiting the zone of interrogation, which demands some specialized reconstruction protocols.

From the position time series, subsequent time differencing yielded instantaneous velocities, which, when averaged at each spatial location over the entire time span of the experiment, yield the ensemble-averaged velocity flow map. The difference between instantaneous and average velocity for each cell yields the fluctuating component of velocity as a time series. This time series was then used to construct the cross-correlation matrix of the velocity components of fluctuations. Trace of this matrix can be interpreted as the total kinetic energy of "turbulence" per unit bulk density, which, when scaled by a constant (the granular temperature, which is equal to two-thirds of the kinetic energy of turbulence), gives the granular temperature of the particulate phase. The error in reconstruction[17] of the tracer particle position has been shown to be less than 5 mm.

CT is a non-invasive technique that is used to measure time-averaged phase holdup profiles in a multiphase system. By placing a strong γ-ray source in the plane of interest and a planar array of scintillation detectors on the other side of the vessel, one measures the attenuation of the beam of γ-radiation. The attenuation is a function of the line-averaged holdup distribution along the path of the beam. Many such "projections" are obtained at different angular orientations around the reactor. The complete set of projections is then used to back-calculate the cross-sectional distribution of densities. Because the density at any point in the cross section is a sum of individual phases weighted by their volume fractions, the cross-sectional distribution of any particular phase can be uniquely recovered. An alternating minimization (AM) algorithm was implemented for CT image reconstruction. The density resolution (as per de Vuono et al.[30]) for the employed CT scanner for a 6-in. column was determined to be 8.1 kg/m^3.

A remark about the uniqueness of the aforementioned experimental systems is appropriate here. For the full characterization of the hydrodynamics in any multiphase flow system with dispersed phases, it is critical to have velocity and holdup information on the *same* unit. One of the main advantages of the CARPT−CT method is that, in the same establishment, both experiments are performed simultaneously and in a *non-invasive* manner, using practically the same hardware and electronics for the two types of measurements. Thus, the techniques can be used to perform consistency checks on each other, as well as benchmark them as other independent experimental techniques. In fact, as shown by Roy et al.,[26,31] it is possible to check the overall mass flux of solids from the consolidated CARPT−CT processed data, from the raw data of CARPT by extracting the solids residence time distribution and then comparing the moments, as well as from an independent measurement of solids flux.[31] The same techniques have been used by Bhusarapu and co-workers.[17,32]

The aforementioned discussion allows for more confidence in the final data. Furthermore, given such consistency checks, CARPT further provides information for higher moments of the flow field (such as kinetic energies, stresses, dispersion coefficients, etc.), which can also be compared with predictions from compatibly high fidelity simulations. In this work, we have made some initial attempts to make comparisons against two-fluid CFD simulations.

3. Two-Phase CFD Modeling

Computational fluid dynamics (CFD) attempts to rigorously solve the conservation laws of mass, momentum, and energy from first principles to yield results at high spatial and temporal resolution. The CFB riser involves dispersed gas−solid flow with very high velocity and strong interphase interactions. In view of the large number of particles in the solids ensemble, the Eulerian−Eulerian two-fluid approach[33,34] has been used. In this approach, both phases are considered to be continuous and fully interpenetrating and both phases are allowed to exist at the same point and at the same time. The probability of finding a phase at a given point in the domain is modeled by the holdup or volume fraction of that phase. More details of the mathematical and theoretical basis of this approach can be found elsewhere.[35,36] The ensemble average of the two-fluid conservation equations leads to the appearance of certain extra terms in the averaged equations, and these must be closed.

Many commercial and public domain two-phase CFD codes have adopted the ensemble-averaged equations. In this work, the ensemble-averaged formulation of the two-fluid equations has been adopted, and the simulations have been performed using the FLUENT library of codes, specifically in Fluent v.6.2.16 (Fluent, Inc., Lebanon, NH).

3.1. Conservation Equations. Ensemble-averaged "two-fluid" conservation equations that represent the most probable or expected flow field are stated as given below.[35,37] The equations assume no mass exchange between the phases:

Continuity (*k*th *phase*)*:*

$$\frac{\partial}{\partial t}(\epsilon_k \rho_k) + \nabla\cdot(\epsilon_k \rho_k \vec{u}_k) = \sum_{p=1}^{n} \dot{m}_{pk} \tag{1}$$

where k = f (for fluid) or s (for solids).

Momentum (*fluid phase*)*:*

$$\frac{\partial}{\partial t}(\epsilon_f \rho_f \vec{u}_f) + \nabla\cdot(\epsilon_f \rho_f \vec{u}_f \otimes \vec{u}_f) = -\epsilon_f \nabla p + \nabla\cdot\bar{\bar{\tau}}_f + \epsilon_f \rho_f \vec{g} + K_{sf}(\vec{u}_s - \vec{u}_f) + \vec{F}_f \tag{2}$$

Momentum (*solids phase*)*:*

$$\frac{\partial}{\partial t}(\epsilon_s \rho_s \vec{u}_s) + \nabla\cdot(\epsilon_s \rho_s \vec{u}_s \otimes \vec{u}_s) = -\epsilon_s \nabla p - \nabla p_s + \nabla\cdot\bar{\bar{\tau}}_s + \epsilon_s \rho_s \vec{g} + K_{sf}(\vec{u}_f - \vec{u}_s) + \vec{F}_s \tag{3}$$

Total volume conservation:

$$\epsilon_s + \epsilon_f = 1 \tag{4}$$

Equation 1 represents the mass balance of each phase with temporal and spatial gradients on the left-hand side and "mass creation" of the *p*th species (in this case, zero) by reaction or phase change. Equations 2 and 3 are momentum conservation equations for the fluid (gas in this case) and solids phase, respectively. The left-hand side represents temporal and spatial transport terms, whereas the right-hand side has terms for the various interaction forces involved. Note that the hydrodynamic pressure is shared by both phases. Hence, the gradient of pressure is pre-multiplied by the respective volume fractions in both equations. Assumption of interpenetrating continua for the discrete solid phase leads to the "solids pressure" term in eq 3, which accounts for normal stresses arising from collisions between individual solid particles. The stress term τ_f in eq 2 represents the shear stress in gas phase. In the solids phase

Table 1. List of Kinetic Theory of Granular Flow (KTGF) Closures

parameter	KTGF correlation used in the CFD model
granular bulk viscosity	$\lambda_s = \frac{4}{3}\epsilon_s\rho_s d_s g_{o,ss}(1+e_{ss})\left(\frac{\Theta_s}{\pi}\right)^{1/2}$
granular conductivity	$k_{\Theta s} = \frac{15 d_s\rho_s\epsilon_s\sqrt{\Theta_s\pi}}{4(41-33\eta)}\left[1+\frac{12}{5}\eta^2(4\eta-3)\epsilon_s g_{o,ss}+\frac{16}{15\pi}(41-33\eta)\eta\epsilon_s g_{o,ss}\right]$ where $\eta = \frac{1}{2}(1+e_{ss})$
granular viscosity	$\mu_s = \frac{4}{5}\epsilon_s\rho_s d_s g_{o,ss}(1+e_{ss})\left(\frac{\Theta_s}{\pi}\right)^{1/2}+\frac{10\rho_s d_s\sqrt{\Theta_s\pi}}{96\epsilon_s(1+e_{ss})g_{o,ss}}\left[1+\frac{4}{5}g_{o,ss}\epsilon_s(1+e_{ss})\right]^2$
radial distribution	$g_{o,ss} = \frac{1}{1-(\epsilon_s/\epsilon_{s,max})^{1/3}}$ where $\epsilon_{s,max} = 0.6$
solids pressure	$P_s = \epsilon_s\rho_s\Theta_s + 2\rho_s(1+e_{ss})\epsilon_s^2 g_{o,ss}\Theta_s$

equation (eq 3), τ_s represents the shear stress term due to collision among the particles.

The terms $K_{sf}(\vec{u}_s - \vec{u}_f)$ and $K_{sf}(\vec{u}_f - \vec{u}_s)$ represent the momentum exchange or "drag" between the two phases in eqs 2 and 3, respectively. These terms are equal in magnitude and opposite in sign, and they account for the friction at the interface between the phases. This term also assumed no acceleration of the relative slip velocity between the phases. The terms $\vec{F}_f$ in eq 2 and $\vec{F}_s$ in eq 3 represent all other forces that may affect the flow, such as electrical, magnetic, and other effects.

3.2. Closures. Examination of the right-hand side of eqs 2 and 3 indicates that closure models are needed to establish relationships among the unknowns so that the set of equations may be solved. The closures used in the current work account for gas−solid drag and solid-phase fluctuations via the kinetic theory of granular flow (KTGF).

3.2.1. Gas−Solids Drag. The drag is an effective way of representing the surface integral of all the forces that exist at the interface between the phases. In a dispersed flow with very high velocity, such as that in the present case, the presence of other particles certainly affects this interaction. However, because the discrete nature of particles is sacrificed in the Eulerian−Eulerian approach, the drag force is modified by some empirical relationship, in terms of Eulerian quantities such as solids holdup. For example, Wen and Yu[23] hypothesized that

$$F_D = F_{DS}\epsilon_f^{-4.7} \tag{5}$$

Therefore, interphase momentum exchange factor appearing in momentum conservation equation becomes

$$K_{s,f} = \frac{3}{4}C_{d,s}\frac{\epsilon_f(1-\epsilon_f)}{d_s}\rho_f\epsilon_f^{-2.65}|\bar{u}_f - \bar{u}_s|$$

$$C_{d,s} = \frac{24}{\epsilon_f Re_s}[1+0.15(\epsilon_f Re_s)^{0.687}] \tag{6}$$

The correlation reported by Wen and Yu[23] is the most commonly used correlation in gas−solid riser literature; hence, to make a base case simulation, the correlation of Wen and Yu[23] was used.

3.2.2. Solid-Phase Fluctuations: Kinetic Theory of Granular Flow (KTGF). To treat the discrete solid phase as the pseudo-continuous one at the reactor scale, the kinetic theory of granular flow (KTGF)[38−41] has been used. Similar to the concept of thermodynamic temperature in classical kinetic theory of gases, the term "granular temperature" is defined to be that which is representative of solid-phase fluctuations. All the granular phase properties, such as solids pressure and solids shear stress, are expressed in terms of granular temperature. Formally, the granular average temperature is defined as[42]

$$\Theta = \frac{2}{3}K_s \tag{7}$$

where Θ is the granular temperature (expressed in units of m^2/s^2) and K_s is the kinetic energy of fluctuations of solids per unit mass. The concept of granular temperature makes it possible to model the granular phase interactions, for which a transport equation of the fluctuating kinetic energy of the granular phase, following Chapman and Cowling,[42] can be represented in the following manner:

$$\frac{3}{2}\left[\frac{\partial}{\partial t}(\rho_s\epsilon_s\Theta_s)+\nabla\cdot(\rho_s\epsilon_s\vec{u}_s\Theta_s)\right] = (-p_s\vec{\vec{I}}+\vec{\vec{\tau}}_s):\nabla\vec{u}_s+\nabla\cdot(k_{\theta_s}+\nabla\Theta_s)-\gamma_{\Theta_s}+\phi_{fs} \tag{8}$$

The left-hand side of this equation represents the transport terms. The first term on the right-hand side represents the production of kinetic energy, because of the interaction between the normal and shear stress matrix with the mean velocity field. The second term on the right-hand side represents the flow of kinetic energy caused by elastic and inelastic collisions between the solid particles. The third term represents the dissipation of kinetic energy due to collisions, whereas the fourth term represents the energy exchange due to interactions with fluid phase fluctuation. Table 1 lists the various closures used for the granular flow quantities.

4. Results and Discussion

In the CREL riser setup, the solids enter through a standpipe inclined at 45°, relative to the main riser section (Figure 1). Visual observation, as well as the experimental CARPT data, suggest that the flow field in the riser section is dominated by

spiraling structures of solids that cross the riser axis.[17] For instance, in the case of the dilute phase transport (DPT) regime, angular normal stress calculated from CARPT data shows a peak in the center of the column, depicting the dominating crossover of spiraling structures across the column.[17] Thus, short of performing the full three-dimensional (3-D) simulation, which is computationally prohibitive at such large vessel sizes, one must formulate a 2-D simulation that respects the presence of these structures and the associated velocity and holdup fluctuations. This is particularly relevant, given the asymmetric solids inlet in the case of the CREL riser (which, incidentally, is typical of many industrial risers).

As a trial, an attempt was made to execute 2-D *axisymmetric* simulation for the current case (the riser itself being cylindrical in shape); however, unrealistically high downward directed solids velocities were obtained at the center of column, and even the mass conservation was not satisfied at the riser scale. The computations clearly were not reliable. Owing to the side entry, solids coming in from the side inlet impinge on the wall directly in front of the inlet, causing the velocity to change direction and swerve upward, being steered by the primary gas flow. This type of motion has been visualized and reported by Roy[43] for liquid−solid flows in risers, and also has been shown through 3-D transient simulations in that type of system. Under the assumption of two-dimensional axisymmetry, this type of phenomenon cannot be simulated, because of the inherent limitation of the geometrical description on the axisymmetric coordinates, which does not respect these 3-D spiraling structures. Therein, the flow is forced to rise upward by preserving centerline symmetry. Clearly, for the considered operating conditions and solids characteristics, the assumption of axisymmetry simply does not permit the incorporation of the motion of 3-D spiraling structures in a 2-D domain.

Strictly, a 3-D transient simulation should be attempted, as outlined by Roy;[43] however, this is prohibitively expensive for the size and dimensions of the system at hand. Thus, with the motivation to describe the flow with fidelity in a 2-D domain, one must resort to a 2-D Cartesian simulation. Such a choice is similar to that of Benyahia et al.[9] and Gomez et al.[44] However, we do recognize the inherent assumption and paradox in our approach. In a 2-D axisymmetric assumption, one is simply azimuthally averaging the 3-D conservation equations and then solving for dependent variables that are averaged in the azimuthal direction. In a 2-D Cartesian simulation of the system at hand, one is essentially describing a "slice" of a 3-D flow (restrained within a cylindrical vessel) using 2-D conservation equations in Cartesian coordinates (which inherently ignore the variation of variables in the third Cartesian dimension, or what is the same as an assumption of spatial periodicity or infinite domain in the third dimension). We make this leap of faith because our visual observation (as well as CARPT data, through the significant presence of the $\tau_{r\theta}$ and $\tau_{\theta z}$ components of solids phase stresses) clearly show that the flow is dominated by spiraling and across-the-centerline movements of the flow structures (initiated by the sideways entry of solids). Thus, a 2-D axisymmetric set of equations that falsely imposes symmetry on the centerline simply is not acceptable.

Table 2 lists the CFD simulation parameters. Uniform velocity profiles were assumed for both the phases at the inlet of the simulated section. In the case of 2-D Cartesian geometry, two symmetric inlets were assumed, one on each side, for the entry of solids to be consistent with the specification of the 3-D cylindrical setup with an asymmetric side inlet. At the wall, a no-slip boundary condition was assumed for the gas phase, whereas the Johnson−Jackson[45] boundary condition was used for the solids phase. To validate the CFD model that is developed, radial profiles of the time-averaged solids velocity and the solids concentration, as well as granular temperature, were compared in the fully developed section.

Table 2. Computational Fluid Dynamics (CFD) Simulation Parameters for the Two-Dimensional (2-D) Cartesian Base Case

parameter	value/comment
Solid Properties	
bulk density	2550 kg/m^3
Sauter mean diameter	150 μm
Model	
Solver	2-D, unsteady
Multiphase	Eulerian−Eulerian
Grid (Base Case)	
radial	15
axial (uniform)	350
Restitution Coefficient	$e = 0.95$, $e_w = 0.90$
granular temperature	1×10^{-5} m^2/s^2
Interphase Interaction	
gas−solid drag closure	Wen and Yu[23]
Inlet Boundary Condition	
gas and solid phases	uniform velocity profile
Outlet Boundary Condition	
gas and solid phases	outflow
Numerical Method	
pressure−velocity coupling	phase-coupled SIMPLE
discretization	second-order UPWIND
Under-Relaxation Parameters	
pressure	0.3
density	1.0
body forces	1.0
momentum	0.1
volume fraction	0.2
granular temperature	0.01
Unsteady Iterations	
time step	0.0001 s
Convergence Criterion	0.001
Initialization	
gas-phase velocity	0
solid-phase holdup	0.0

This is the first time that CFD simulations are being validated against the data obtained from non-invasive CARPT−CT techniques for a gas−solids system. Earlier, Sanyal et al.[2] compared turbulent kinetic energy profiles, in addition to the mean liquid velocity and mean gas hold-up profiles, obtained from CFD simulations to CARPT−CT experimental data for a bubble column (gas−liquid system). Much better agreement was observed for the turbulent parameters, and authors have recommended further improvement in the turbulence model. In fluidization literature, until now, the general trend has been to match the averaged flow behavior, which essentially refers to the mean solids velocity profile and mean solids volume fraction profile in the cross-flow direction.

We feel that the next phase of development in the two-fluid modeling of the gas−solids flows would come from our ability to predict the profiles of higher moments of velocity and velocity fluctuations, such as kinetic energies of fluctuations and shear stresses in the solids assembly. As such, if it were possible to match all moments of velocity fluctuations with the corresponding experimental profiles, then the model would be perfect. Although it would be a search for the "holy grail" of two-phase CFD, as of now, we are taking the next step in comparing profiles of solids granular temperature (which is directly related to the solids fluctuating kinetic energy).

4.1. Fast Fluidization (FF). For the fast fluidization (FF) regime of flow, the operating conditions considered were as

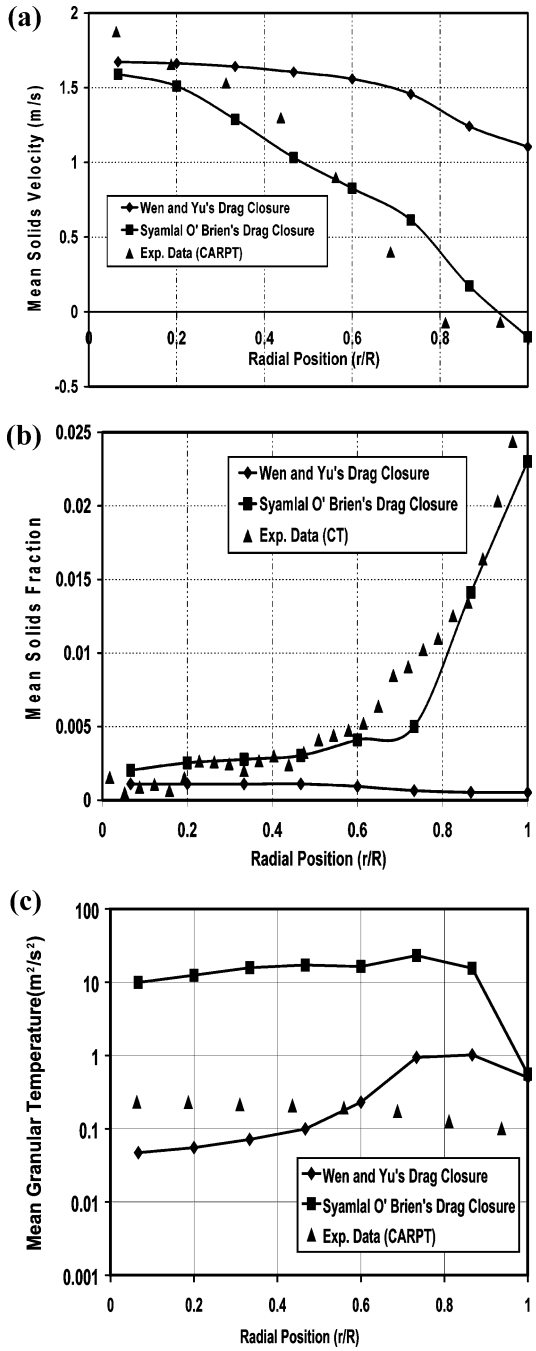

Figure 2. (a) Comparison of radial profile of mean solids velocity for $U_g = 3.2$ m/s and $G_s = 26.6$ kg/m^{2}s (FF regime). (b) Comparison of radial profile of mean solids fraction for $U_g = 3.2$ m/s and $G_s = 26.6$ kg/m^{2}s (FF regime). (c) Comparison of radial profile of mean granular temperature for $U_g = 3.2$ m/s and $G_s = 26.6$ kg/m^{2}s (FF regime).

follows: $U_g = 3.2$ m/s, $G_s = 26.6$ kg/m^{2}s. Figure 2 shows the base-case simulation results with parameters listed in Table 2 and with Wen and Yu[23] drag closure (eq 6). The velocity profile predicted was much more uniform, when compared to the experimental data, and the values in the annular region were overpredicted. Improvement in the flow prediction can be obtained by choosing the "best-suited" closures for the various interactions involved. In the case of gas−solids dispersed flow, among various interactions, gas−solid drag (which accounts for the interphase interaction between mean velocity fields) is the dominant one. Therefore, subsequent simulations were attempted with different drag closure (such as that reported by Syamlal and O'Brien[22]).

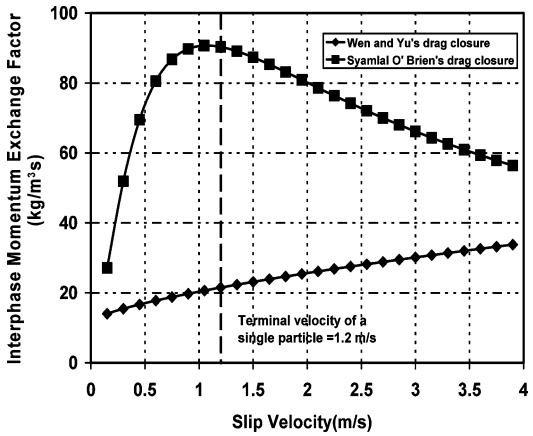

Figure 3. Comparison of interphase momentum exchange factor predicted by Wen and Yu's[23] drag closure and the Syamlal−O'Brien[22] drag closure (at a constant solids fraction of 0.1%) versus slip velocity.

According to this, the interphase momentum exchange factor is given by

$$K_{s,f} = \frac{3\epsilon_s\epsilon_g\rho_g}{4{v_{r,s}}^2 d_s} C_{d,s}\left(\frac{Re_s}{v_{r,s}}\right)|\bar{u}_s - \bar{u}_g| \tag{9}$$

where

$$C_{d,s} = \left(0.63 + \frac{4.8}{\sqrt{Re_s/v_{r,s}}}\right)^2$$

$$v_{r,s} = 0.5[A - 0.06Re_s + \sqrt{(0.06Re_s)^2 + 0.12Re_s(2B - A) + A^2}]$$

$$A = \epsilon_g^{4.14}$$

$$B = 0.8\epsilon_g^{1.28}$$

$$B = \epsilon_g^{2.65}$$

Figures 2a and 2b show that the Syamlal−O'Brien drag closure[22] predicts mean solids flow behavior with much more fidelity. However, a larger discrepancy is observed in the granular temperature (Figure 2c). The typical characteristic of the FF regime under low flux conditions is a downflow of solids at the wall, which is predicted with fidelity using the Syamlal−O'Brien drag closure.[22] The drag expression accounts for increased volume loading through the use of a drag coefficient that is dependent on volume-fraction-dependent terminal velocities. Because the FF regime is characterized with relatively nonuniform holdup, a volume-fraction-dependent drag coefficient might be a considerable improvement in predicting the experimental data.

Inspection of Figure 3 reveals that the cross-sectional averaged slip velocity predicted by the current simulation work is within the range of the particle terminal velocity ($U_t = 1.2$ m/s) and is in agreement with earlier studies.[14] Figure 3 compares the interphase momentum exchange factors that are predicted by the drag closures reported by Wen and Yu[23] and Syamlal and O'Brien[22] at a solids volume fraction of 0.1%. The interesting particular feature to be noted is that, unlike Wen and Yu's[23] drag closure, Syamlal and O'Brien's[22] drag closure shows two distinct regions. In one region, the slip velocity is less than the terminal velocity of a single particle, where interphase momentum exchange increases with increasing slip velocity. In the other region, where the slip velocity is higher

than the single particle terminal velocity, a decrease in interphase momentum exchange with increasing slip velocity is predicted. In effect, although (Wen and Yu[23]) the interphase drag force scales monotonically with slip velocity, the latter model predicts that, within a cluster (wherein effective slip velocity is higher than the single particle terminal velocity), the drag will be effectively reduced.

Earlier, Matsen[46] reported that in the FF regime (in which slip velocities are higher than the single terminal velocity), drag force decreases with increasing slip velocity. The Syamlal−O'Brien[22] drag closure captures this observation, which suggetss that it has relatively "better" performance. Another point of particular significance is the relative magnitude of the drag force to adhesive forces for group B particles in the FF regime. This issue requires further investigation, and there is a need to formulate closure forms that explicitly account for this fact.

The granular temperature predicted by the Syamlal−O'Brien[22] drag closure is on the order of 20 m^2/s^2, whereas Wen and Yu's[23] drag closure predicts average values of ∼0.35 m^2/s^2, versus experimentally (CARPT) observed values of 0.2 m^2/s^2 (see Figure 2c). This discrepancy is most likely because of the fact that the granular temperature models fluctuations in solids velocity, under the assumption that the fluctuating kinetic energy has a Maxwellian distribution (inherent in the kinetic theory approaches). This assumption may no longer be valid for the current operating conditions.

4.2. Dilute Phase Transport (DPT). Comparisons were also made between the CFD model and experimental data in the dilute phase transport (DPT) regime of flow. For the DPT regime, two operating conditions were chosen: $U_g = 3.9$ m/s and $G_s = 33.7$ kg/m^2s, and $U_g = 4.5$ m/s and $G_s = 36.8$ kg/m^2s. Figures 4 and 5 show the comparison of simulated flow behavior with the experimental data. Simulations were performed with Wen and Yu's[23] drag closure as well as the Syamlal−O'Brien[22] drag closure. It can be seen that, although both the drag closures do capture the order of magnitude of the experimental values, both of the drag closures underpredict the mean solids velocity. Since DPT is a relatively uniform regime, a volume-fraction-dependent drag coefficient is not a huge improvement over the single-particle drag closures.

The average slip velocity predicted for both of the operating conditions by both drag closures is ∼2 m/s (∼1.5 times greater than the single-particle terminal velocity). The predicted granular temperature is ∼1 order of magnitude higher than the experimentally observed values. Thus, in both flow regimes, the granular temperature (i.e., the fluctuating kinetic energy of solids) is overpredicted. One possible reason for this overprediction is the fact that the CARPT-measured granular temperature values are azimuthally averaged, whereas the CFD-predicted granular temperature values are not. Peirano et al.[16] showed that, for Geldart[10] group B particles, as the fluidization velocities increases, the role of the mean gas solid interactions in energy dissipation becomes dominant. Yasuna et al.[47] performed CFD simulation for the fully developed region of a gas solid riser, for various experimental data that are available in the literature, using the model reported by Sinclair and Jackson.[6] In that study, CFD simulation predictions were in much better agreement with the experimental data for gas solids flow with Geldart[10] group A particles, as compared to that with Geldart[10] group B particles. Thus, certainly, KTGF closures must be appropriately modified for the FF regime of operation of Geldart group B particles. This issue will be presented in detail in a future contribution.

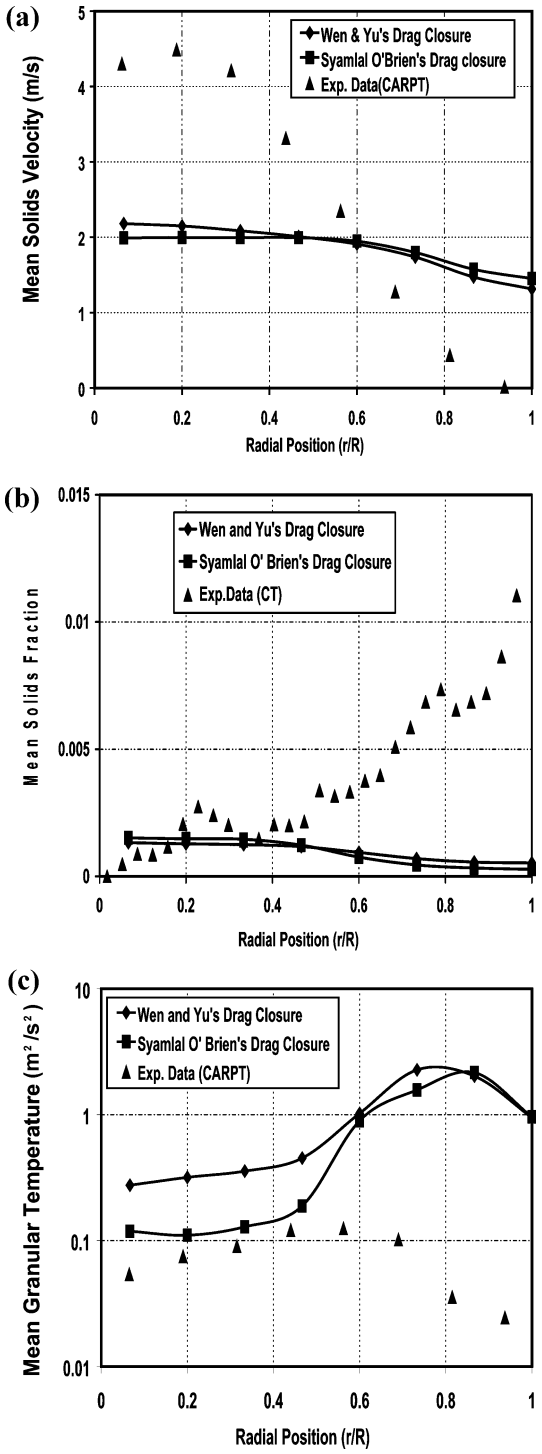

Figure 4. (a) Comparison of radial profile of mean solids velocity for $U_g = 3.9$ m/s and $G_s = 33.7$ kg/m^2s (DPT regime). (b) Comparison of radial profile of mean solids fraction for $U_g = 3.9$ m/s and $G_s = 33.7$ kg/m^2s (DPT regime). (c) Comparison of radial profile of mean granular temperature for $U_g = 3.9$ m/s and $G_s = 33.7$ kg/m^2s (DPT regime).

5. Conclusions

In the present study, a two-dimensional (2-D) Cartesian computational fluid dynamics (CFD) model was developed for a pilot-plant-scale gas−solids circulating fluidized-bed (CFB) riser with the currently available closures. Simulation results were compared with experimental data obtained from noninvasive techniques such as computer automated radioactive particle tracking (CARPT) and computed tomography (CT). To capture the multiscale phenomena with more fidelity, the granular temperature has also been compared. It was found that

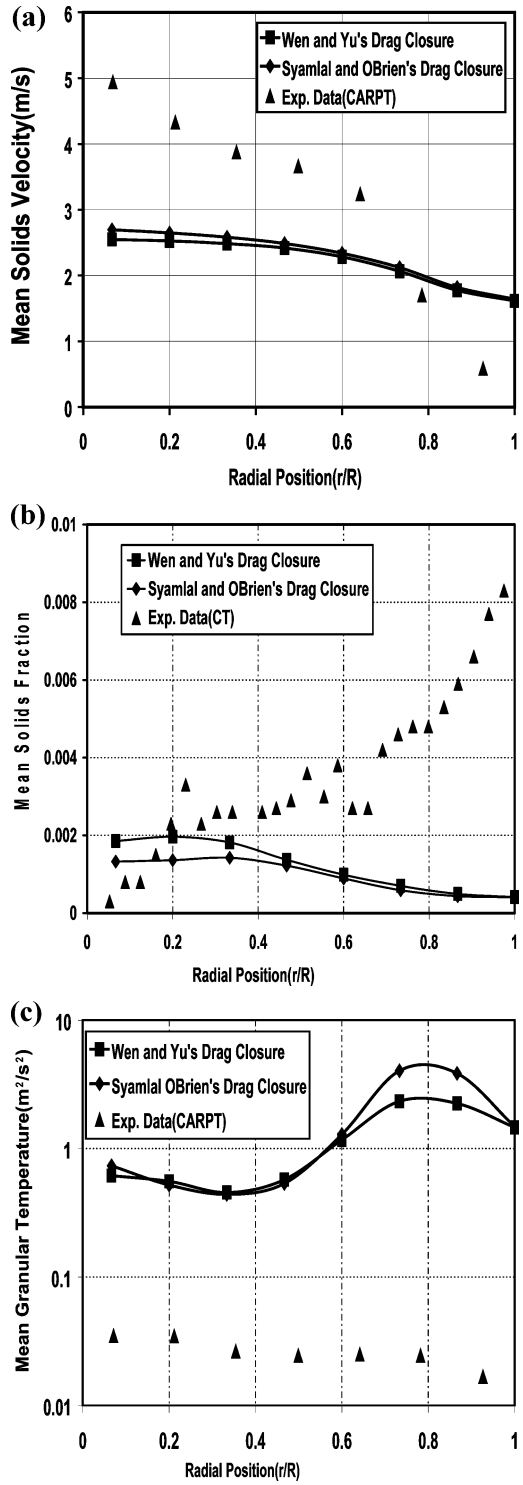

Figure 5. (a) Comparison of radial profile of mean solids velocity for U_g = 4.5 m/s and G_s = 37 kg/m^{2}s (DPT regime). b. Comparison of radial profile of mean solids fraction for U_g = 4.5 m/s and G_s = 37 kg/m^{2}s (DPT regime). c. Comparison of radial profile of mean granular temperature for U_g = 4.5 m/s and G_s = 37 kg/m^{2}s (DPT regime).

Wen and Yu's[23] drag closure underpredicts the mean solids velocity profile for both "fast fluidization" (FF) and "dilute phase transport" (DPT) regime. For the FF regime, the Syamlal−O'Brien[22] drag closure, which was based on the volume-fraction-dependent drag coefficient, was determined to be acceptable and predictive.

In this contribution, we have also presented comparisons of the two-fluid model predictions with granular temperature profiles for the solids phase. Quite honestly, our predictions of this "second moment" of velocity correlations (kinetic energy of granular flow, or granular temperature) leaves much to be desired and points toward the development of better closures for predicting the fluctuations. However, we wish to publish these results in the open literature for researchers to take this up as a challenge for benchmarking their two-phase CFD work, just as we are undertaking. We believe that, for further improvement in gas−solids CFD models, we must benchmark our models, not only against profiles of mean velocity and holdup, but also against the higher moments of fluctuations. To the best of our knowledge, our present contribution is the first reported attempt at this in riser flow, and points to the versatility of the CARPT−CT techniques for serving to generate benchmark data for "higher-order" CFD model validation.

Furthermore, it can be stated that, for further improvement in closures for the flow of Geldart[10] group B particles, one would also need to model the relative importance of surface (adhesive) forces (vis-à-vis, the drag formulation). The incorporation of the role of surface forces in the modified kinetic theory of granular flow (KTGF) closures may lead to better prediction of the granular phase temperature. A full three-dimensional (3-D) transient simulation in a relatively smaller system might be useful to study the role of spiraling structures and their role on flow development. This work is currently underway.

Nomenclature

$C_{d,s}$ = single-particle drag coefficient
D = diameter of the column (m)
d_s = particle diameter (m)
e = restitution coefficient
F_D = drag force on multiple particles (N)
F_{D_s} = drag force on single particles (N)
G = solids mass flux (kg/m^{2}s)
$g_{o,ss}$ = radial distribution function
k_{Θ_s} = diffusion coefficient (kg/ms)
$K_{s,f}$ = interphase momentum exchange factor (kg/m^{3}s)
p = pressure (N/m^2)
Re = Reynolds number
t = time (s)
U = superficial velocity (m/s)
u = velocity (m/s)
U_t = terminal velocity (m/s)
z = axial distance (m)

Greek Symbols

Θ = granular temperature (m^2/s^2)
ϵ = volume fraction
γ = collisional dissipation of granular temperature (J/m^{3}s)
λ = granular bulk viscosity (kg/ms)
τ = shear stress (N/m^2)
μ = viscosity (kg/ms)
ϕ = energy exchange per unit volume between two phases (J/m^{3}s)

Subscripts and Superscripts

g = gas phase
s = solid, granular

Literature Cited

(1) Grace, J. F. High velocity fluidized bed reactors. *Chem. Eng. Sci.* **1990**, *45*, 1953−1966.

(2) Sanyal, J.; Vàsquez, S.; Roy, S.; Dudukovic, M. P. Numerical simulation of gas−solid dynamics in cylindrical bubble column reactors. *Chem. Eng. Sci.* **1999**, *54*, 5071−5083.

(3) Ding, J.; Gidaspow, D. A bubbling fluidization model using kinetic theory of granular flow. *AIChE J.* **1990**, *36*, 523−538.

(4) Wachem, B. G. M.; van Schouten, J. C.; Bleek, C. M. van den Krishna, R.; Sinclair J. L. Comparitive analysis of CFD models of dense gas−solid systems. *AIChE J.* **2001**, *47* (5), 1035−1050.

(5) Du, W.; Bao, X.; Xu, J.; Wei, W. Computational fluid dynamics modeling of spouted bed: Assessment of drag coefficient correlations. *Chem. Eng. Sci.* **2006**, *61*, 1401−1420.

(6) Sinclair, J. L.; Jackson, R. Gas−particle flow in a vertical pipe with particle−particle interactions. *AIChE J.* **1989**, *35*, 1473−1486.

(7) Neri, A.; Gidaspow, D. Riser hydrodynamics: simulation using kinetic theory. *AIChE J.* **2000**, *46* (1), 52−67.

(8) Pita, J. A; Sundaresan, S. Developing flow of a gas−particle mixture in a vertical riser. *AIChE J.* **1993**, *39*, 541−552.

(9) Benyahiya, S.; Arastoopour, H.; Knowlton, T. M.; Massah, H. Simulation of particles and gas flow behavior in the riser section of fluidized bed using the kinetic theory approach for the particulate phase. *Powder Technol.* **2000**, *112* (1−2), 24−33.

(10) Geldart, D. Types of gas fluidization. *Powder Technol.* **1973**, *7*, 285−292.

(11) Basu, P. Combustion of coal in CFB boiler: A Review. *Chem. Eng. Sci.* **1999**, *54*, 5547−5557.

(12) Yerushalmi, J.; Avidan, A. A. High Velocity Fluidization. In *Fluidization*, Second Edition; Davidson, J. F., Clift, R., Harrison, D., Eds.; Academic Press: New York, 1985.

(13) Horio, M.; Kuroki, H. Three-dimensional flow visualization of dilutely dispersed solids in bubbling and circulating fluidized beds. *Chem. Eng. Sci.* **1994**, *49*, 2413−2421.

(14) Balasubramaniyan, N.; Kannan, C. S. Slip velocity characteristics in the riser of circulating fluidized bed. *Chem. Eng. Technol.* **1997**, *20*, 491−494.

(15) Molerus, O. Interpretation of Geldart's type A, B, C & D powders by taking into account interparticle cohesion forces. *Powder Technol.* **1982**, *33*, 81−87.

(16) Peirano, E.; Palchonok, G.; Johnsson, F.; Leckner, B. Estimates of turbulence mechanisms in circulating fluidized bed combustors. *Powder Technol.* **1998**, *96*, 90−105.

(17) Bhusarapu, S. Solids flow mapping in a gas−solid riser, D.Sc. Thesis, Washington University, St. Louis, MO, 2005.

(18) Tsuji, Y.; Morikawa, Y.; Shiomi, H. LDV measurements of an air−solid two-phase flow in a vertical pipe. *J. Fluid Mech.* **1984**, *139*, 417−437.

(19) Luo, K. M. Dilute, dense-phase and maximum solid−gas transport, D.Sc. Thesis, Illinois Institute of Technology, Chicago, IL, 1987.

(20) Mathiesen, V.; Solberg, T.; Hjertager, B. H. An experimental and computational study of multiphase flow behavior in a circulating fluidized bed. *Int. J. Multiphase Flow* **2000**, *26*, 387−419.

(21) Ibsen, C.; Solberg, T.; Hjertager, B. H. A study of dilute to dense flow in a circulating fluidized bed. Presented at the International Symposium on Multiphase Flow Transport Phenomena (MFTP-2000), November 5−10, 2000, Antalya, Turkey.

(22) Syamlal, M.; O'Brien, T. J. Computer simulation of bubbles in a fluidized bed. *AIChE Symp. Ser.* **1989**, *85*, 22−31.

(23) Wen, C. Y.; Yu, Y. H. Mechanics of fluidization. *Chem. Eng. Prog. Symp. Series* **1966**, *62*, 100−111.

(24) Nieuwland, J. J.; van Sint Annaland, M.; Kuipers, J. A. M.; van Swaaij, W. P. M. Hydrodynamic modeling of gas/particle flows in riser reactors. *AIChE J.* **1996**, *42* (6), 1569−1582.

(25) Zhang, Y.; Reese, J. M. The drag force in two-fluid models of gas−solid flows. *Chem. Eng. Sci*. **2003**, *58* (9), 1641−1644.

(26) Roy, S.; Kemoun, A.; Al-Dahhan, M. H.; Duduković, M. P. Experimental investigation of hydrodynamics in a liquid solid riser. *AIChE J.* **2005**, *51* (3), 802−835.

(27) Bhusarapu, S.; Al-Dahhan, M. H.; Duduković, M. P. Solids flow mapping in a gas-solid riser: mean holdup and velocity fields. *Powder Technol.* **2006**, *163* (1−2), 98−123.

(28) Degaleesan, S. Fluid dynamic measurements and modeling of liquid mixing in bubble columns, D.Sc. Thesis, Washington University, St. Louis, MO, 1997.

(29) Pan, Y; Duduković, M. P.; Chang, M. Numerical investigation of gas driven flow in 2-D bubble columns. *AIChE J.* **2000**, *46* (3), 434−449.

(30) De Vuono, A. C.; Schlosser, P. A.; Kulacki, F. A.; Munshi, P. Design of an isotopic CT scanner for two phase flow measurements. *IEEE Trans. Nucl. Sci.* **1980**, *NS27-1*, 814−820.

(31) Roy, S.; Kemoun, A.; Al-Dahhan, M.H.; Duduković, M. P. A method for estimating the solids circulation rate in a closed-loop circulating fluidized bed. *Powder Technol.* **2005**, *44*, 9739−9749.

(32) Bhusarapu, S.; Fongerland P.; Al-Dahhan, M. H.; Duduković, M. P. Measurement of overall solids mass flux in a gas solid circulating fluidized bed. *Powder Technol.* **2004**, *148* (2−3), 155−168.

(33) Anderson, T. B.; Jackson, R. A fluid mechanical description of fluidized beds: stability of the state of uniform fluidization. *Ind. Eng. Chem. Fundam.* **1968**, *7*, 12−21.

(34) Harlow, F. H.; Amsden, A. A. Numerical calculation of multiphase fluid flow. *J. Comput. Phys.* **1975**, *17*, 19−52.

(35) Drew, D. Mathematical modeling of two-phase flow. *Ann. Rev. Fluid Mech.* **1983**, *15*, 261−291.

(36) Drew, D. A.; Joseph D. D.; Passman, S. L. *Particulate Flows: Processing and Rheology*; Springer: Berlin, 1998.

(37) Kashiwa, B. A.; Gore, R. A. A Four-Equation Model for Multiphase Turbulent Flow. Presented at the First Joint ASME/JSME Fluids Engineering Conference, 1991.

(38) Bagnold, R. A. Experiments on a gravity-free dispersion of large solid spheres in a newtonian fluid under shear. *Proc. R. Soc. London A* **1954**, *A225*, 49−63.

(39) Savage, S. B.; Jeffrey, D. J. The stress tensor in a granular flow at high shear rate. *J. Fluid Mech.* **1981**, *140*, 255−272.

(40) Jenkins, J. T.; Savage, S. B. A theory for the rapid flow of identical, smooth, nearly elastic spherical particles. *J. Fluid Mech.* **1983**, *130*, 187−202.

(41) Lun, C. K. K.; Savage, S. B.; Jeffrey, D. J.; Chepurniy, N. Kinetic theories for granular flow: inelastic particles in couette flow and slightly inelastic particles in a general flow field. *J. Fluid Mech.* **1984**, *140*, 223−256.

(42) Chapman, S.; Cowling, T. G. *The Mathematical Theory of Non-uniform Gases*, 3rd Edition; Cambridge University Press: Oxford, U.K., 1990.

(43) Roy, S. Quantification of two phase flow in liquid-solid risers, D.Sc. Thesis, Washington University, St. Louis, MO, 2000.

(44) Gomez, L. C.; Miloli, F. E. Numerical study on the influence of various physical parameters over the gas−solid two-phase flow in the 2D riser of a circulating fluidized bed. *Powder Technol.* **2003**, *132*, 216−225.

(45) Johnson, P. C.; Jackson, R. Frictional−collisional constitutive relations for granular material with application to plane shearing. *J. Fluid Mech.* **1987**, 176, 67.

(46) Matsen, J. Mechanisms of choking and entrainment. *Powder Technol.* **1982**, *32*, 21−33.

(47) Yasuna, J. A.; Moyer, H. R.; Elliott, S.; Sinclair, J. L. Quantitative predictions of gas particle flow in a vertical pipe with particle-particle interactions. *Powder Technol.* **1995**, *84*, 23−34.

Received for review January 13, 2007
Revised manuscript received August 17, 2007
Accepted August 28, 2007

IE0700819